NUMERICAL ANALYSIS OF THERMALLY-INDUCED RESIDUAL STRESS AND DEFLECTION OF CFRP WING STRUCTURE

Shijun Guo, Wenli Liu* and Prahchaya Paophongnbuam

Centre of Aeronautics, Cranfield University, Cranfield MK43 0AL, UK
Corresponding author (wenli.liu@cranfield.ac.uk)

Keywords: Effective temperature difference, Thermally-induced residual stress, Deflection, FEA, Composite wing

ABSTRACT

The thermally-induced residual stress and the corresponding deflection of the carbon fibre reinforced plastics (CFRP) unsymmetrical laminate, stiffened panel and the integrated wing structure were studied through Finite Element Analysis (FEA). An unsymmetrical laminated sample was manufactured and the deflection was measured using co-ordinate measurement machine (CMM). By calibrating the FEA results, the corresponding stress showed that either linear or non-linear analysis could be used and the important parameter of effective temperature difference was determined. Stiffeners were then added to the flat laminate model and the results showed an increase in the panel stiffness causing an increase in thermal stresses and a reduction of the maximum deflection of the panel. The knowledge and the results carried out from the two analyses were finally used for a wing structure model. By applying three different boundary conditions, the results showed that the stress is at maximum when the wing is fully clamped at the spars on one end, whereas the thermal stress between components reduces if the wing is allowed to freely deform when cured, resulting in large deformation of the overall structure.

1 INTRODUCTION

Carbon Fibre Reinforced Plastics (CFRP) has not only superior material properties such as very high specific stiffness and strength, but also unique directional stiffness and strength over metallic materials. This offers a potential for structure tailoring to meet special design requirements. For aerospace engineers, it is feasible to design a much stronger, reliable and lighter aircraft structure in order to satisfy the needs in the competitively growing market. However, apart from the fundamental understanding of the interactions between the constituent materials, it is also important for the engineers to consider the environment impact especially thermal effect on the material properties and structure behaviour in order to create a reliable design. Such thermal impact could occur during operational service or during manufacture curing process. It can give rise to unfavourable internal stress which is commonly referred to as residual stress and become a negative factor for damage tolerance and fatigue failure as well as significant shape distortion.

This investigation concerns the thermal residual stress and shape distortion of laminated composite structure due to manufacturing process. Unlike the metallic components where post-process treatments can be adopted to eliminates/minimize the residual stress and the distortion effects, larger safety margin is taken in composite structure design along with the constraint of symmetric laminate to prevent uncertainties. However, this approach is at the cost of structural weight and manufacture options.

While the effect of thermal residual stress on a single unit composite structure is well studied [1-4], few works explore the thermal effects of integrated composite structures such as wing box structure by co-curing manufacture process. This is an interesting aspect opens to a design approach to include the manufacturing factors as well as part of the optimization process.

2 METHODOLOGY

2.1 Effective temperature difference

It is assumed that composite are not fully hardening after the end of the curing process and that there are still changes in the mechanical properties which can have an impact on the stiffness and so the thermally-induced residual stress. If ignoring this assumption and taking the change of temperature to start from the "curing temperature" which is given by the material manufacturer, this can over predicts the stress level. Therefore to compensate this effect, a lower temperature difference ΔT should be used in order to simulate the composites cooling effects using FEA.

The paper proposes a parameter of effective temperature difference ΔT_{ETD} , which is not the actual curing temperature difference used in coupon manufacture. The value will be obtained through simulations and validations of the thermally-induced residual deflection. It should therefore be clear that the research work presented in the paper does not aim to simulate the resin transition from rubbery to glassy state. It is also beyond the scope of the work presented to determine the amount of residual stress which is generated purely due to the chemical aspects because the chemical shrinkage effect can be ignored according to previous research [5].

This is due to the fact that it is intended to observe a clear relationship between the effects of the thermal residual stress and the thermal loadings on the unconstrained panel using an unsymmetrical laminate. If symmetrical laminate is used, a curved geometry must be manufactured and the spring-in effect [3] must be studies instead. This requires a more complex analysis which is considered to be unnecessary for this project.

2.2 Deflection measurement

The co-ordinate measurement machine (CMM) of Rennishaw Cyclone 3D Scanning System was used to produce the digitised deflection of coupons by measuring the three dimensional co- ordinates of the entire coupon surfaceThe experimental analysis is based on the measurements of the deflections at various locations of the panels in order to use it to validate the FEA results. An unsymmetrical laminated coupon was manufactured for CMM. The machine uses a contacting probe as a method of measurement at which the profiles of the plate is then precisely scanned within the maximum of 1.0 mm tolerance and replicates as 3D point cloud stored as a certain file format. These points are classified as a primary data and then processed to catia display.

.

2.3 Numerical models

The entire process of the FEA was achieved in the commercial package of MSC. Patran/Nastran. With the applied boundary conditions, the stresses (σ_x, σ_y, τ_{xy}) for each of the plies and the overall displacement (δ) were obtained and compared. The three FE models are described here together with different boundary conditions, of which the effects on the thermal residual stress and deflection will be presented in the next section of results.

Unsymmetrical laminate

A study of a simple geometric laminate was carried out at which the results predicted by the FEA are validated by the experimental data. It should be specified here that the unsymmetrical laminates are especially selected for this analysis. This is due to the fact that it is intended to observe a clear relationship between the effects of the thermal residual stress and the thermal loadings on the unconstrained panel using a simple flat laminate. Cooling temperature difference is applied in FEA and the mechanical material properties including coefficient of thermal expansion are the part of necessary input data to simulate the thermal cooling process.

To validate the results of the FE analysis in order to be used for design of more complex geometries, the FE model of the flat unsymmetrical laminate were constructed. Based on the unsymmetrical sample, the laminates will be used to study the effect of thermal residual stress in the 'freely deformed laminate'. By assigning the relevant loading conditions and conducting both linear

and non-Linear static analysis, the deflection and the stresses in the laminates are validated against the numerical and experimental results.

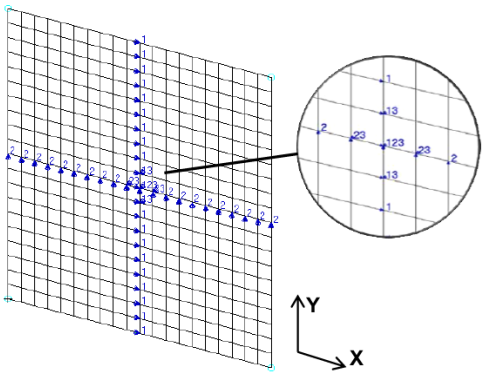

Figure 1: Constraints applied to the flat model

To model the simple flat laminate, CQUAD4 shell elements were used. The meshing follows the mesh seeds which are planted along the edges, resulting in 20 elements along the edges and the total of 400 elements for the entire laminate. The boundary conditions are used in such a way that the minimum constraints are being applied to the model and that no unwanted stress will be generated during the thermal analysis. The constraints applied are as shown in Fig. 1, where the numbers 1, 2 and 3 indicates that the nodes are being restricted to move in the x, y and z direction respectively. This allows the model to fully contracts and expands during the thermal analysis without generating any undesirable stress.

Thermal loading was then introduced in order to simulate the cooling phase of the curing cycle. As the laminates were cured by an initial temperature of 180°C and final temperature of 25°C which corresponds to the actual manufacturing conditions, resulting in the actual temperature difference ΔT_{ACTUAL} is equal to -155°C. As the laminates are relatively thin, the temperature was assigned uniformly to all of nodes assuming that the cooling rate at the top and bottom surfaces is equal throughout the manufacturing process.

In order to find the best suitable effective temperature difference ΔT_{ETD}, the model was kept final temperature at 25°C and varied the initial temperature from 180 down to 100°C. By running the analysis using variable ΔT, the maximum deflections at each of the analysis were then obtained and compared with the actual maximum deflection of the coupon measured using CMM. The best suitable effective temperature difference ΔT_{ETD} was then determined, which would be used for the following stiffened panel and wing structure studies.

Stiffened panel

The analysis of stiffened panel aims to identify the effect caused to the CFRP panel due to the implementation of the stiffeners. Figure 2 illustrated a small section of the wing stiffened panel with I shape stiffeners. The panel was modelled by shell elements CQUAD, by which the overall panel displacement and stress in relevant plies were then compared together with different boundary conditions. The stacking sequence of the skin was kept the same as the unsymmetrical laminate presented in Section 3.1, whereas the stiffener has a symmetrical layup. It is worthwhile to note that the value of effective temperature difference ΔT_{ETD} obtained from the correlation study of the unsymmetrical laminate was consistently applied to this stiffened panel model and the following wing structure.

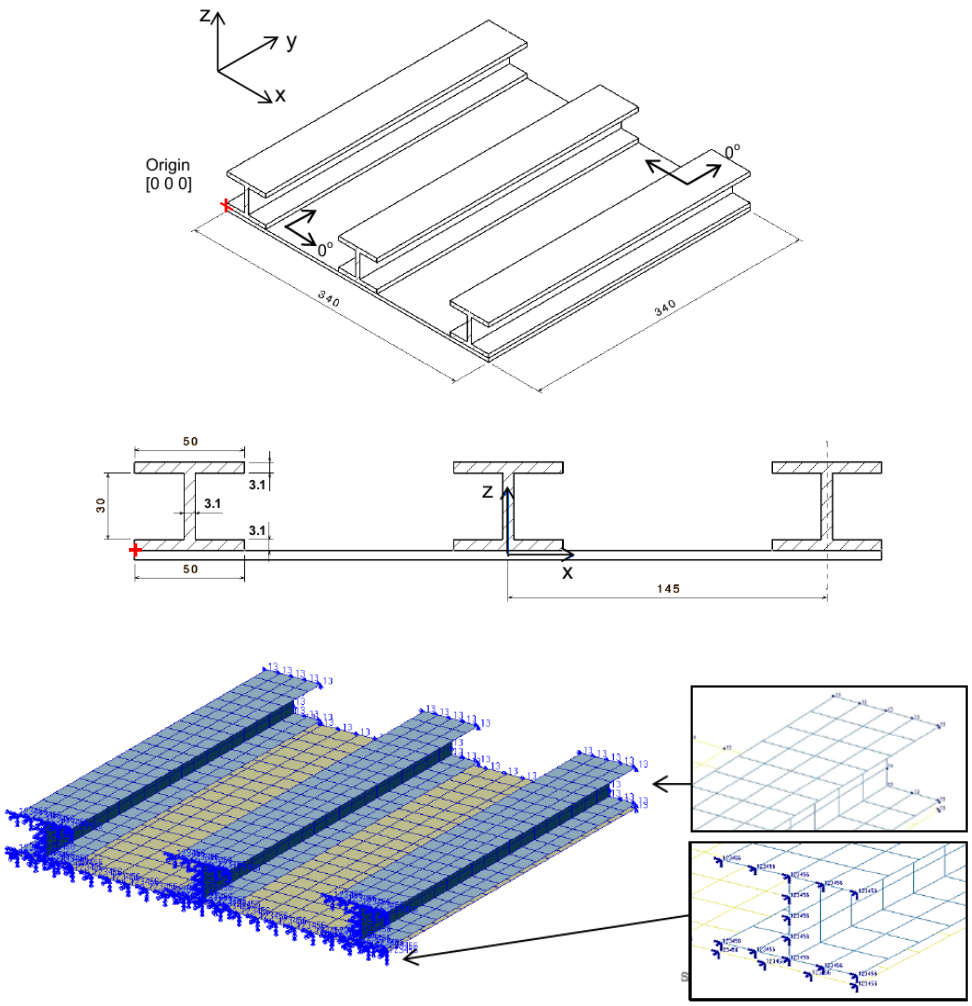

Figure 2: Configuration of the Skin-Stringer model. (all dimensions are in mm)

The effect of applicable boundary conditions on the thermally-induced residual stress and deflections for the stiffened panel were also studied by the FE model. Two cases are specified as follows,

Case 1 constraint: Fixed Boundary conditions applied at the stringer ends as well as the top and bottom edges of the panel restricting all nodes' translational [T1 T2 T3 R1 R2 R3]. This represents that the skin-stringer section was clamped at the end while undergoes thermal cooling.

Case 2 constraint: The Fixed boundary conditions [T1 T2 T3 R1 R2 R3] are applied to the stringer and the panel at the bottom edge as shown in Fig 2. At another side (top edge), the panel are allowed to deform and that the restriction are only for T1 and T3. This represent that the stiffened panel are clamped at one of the edges and that allowing free extension at another.

Wing structure

A typical geometry of the wing model was used to represent wing structures. The aim of this analysis is to observe the thermal residual stress and the strain developed between different wing's components during the manufacturing composite wing. Figure 3 shows the inner wing of 16700 mm length including 2 C-sectioned spars, 14 ribs, 10 stiffeners, and bottom wing cover skins, where the stacking sequences of all the components are kept symmetrical to satisfy current industrial baseline design. Briefly, the wing structure was modelled by shell elements again and the thermal loading was applied with the same ΔT_{ETD} as the previous two models.

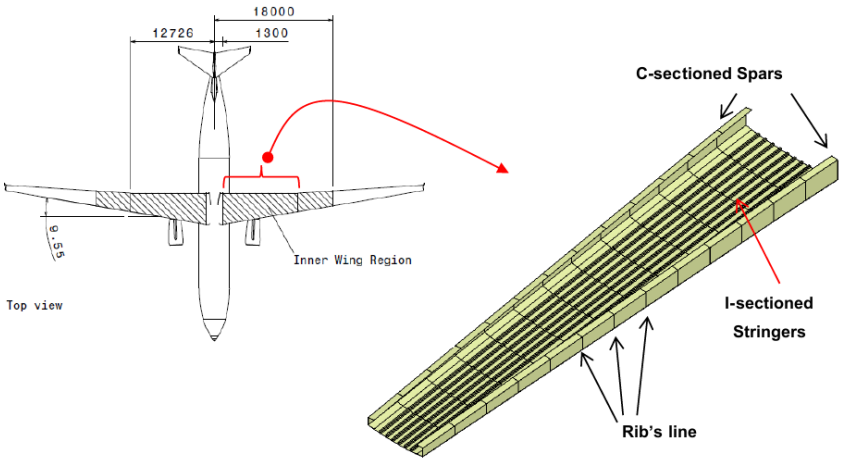

Figure 3: Geometry of wing structure.

Three different boundary conditions were applied to the FE model to quantify the influence on the thermally-induced residual stress and deflections.

Case 1 constraint: The nodes representing the Skin, Spars and Stringers are fixed in translation at one of the wing end (root) [T1 T2 T3 R1 R2 R3]. This is the typical boundary conditions which will be used for the analysis of the wing when subjected to airload.

Case 2 constraint: Similar to the Case 1 constraint, the constraint for case 2 will be applied to the spars instead.

Case 3 constraint: Constraint applied to a single node will be used at which all motioned will be restricted [T1 T2 T3 R1 R2 R3]. This represents the wing when it undergoes thermal cooling inside the autoclave without any supported from external tools (clamped). The wing geometry is then said to be freely deformed.

3 RESULTS AND DISCUSSION

3.1 Correlation of flat laminates

The composite material used for FEA and testing samples is aerospace standard CFRP of M21/T800S with the material properties shown in Table 1. The unsymmetrical laminate has 16 plies with the stacking sequence of [45/0/-45/90/45/0/-45/90/90/45/0/-45/90/45/0/-45] with a size 340 mm x 340 mm. The total thickness of the laminates is 4.192 mm. It should be specified here that the unsymmetrical laminates are especially selected for this analysis.

Table 1: Material properties of CFRP of M21/T800S

Name	Hexply M21/35%/268/T800S				
Fibre	Toray T800S				
Matrix	M21 Epoxy resin				
Density	ρ	1.58×10^{-9}	tonne/mm^3		
Ply thickness	t	0.261	mm		
Resin ratio	V_r	0.35			
Elastic Modulus			E_{11}	172	GPa
			E_{22}	8.5	GPa
Shear Modulus			G_{12}	5	GPa
Poisson ratio			ν_{12}	0.35	
CTE			α_{11}	-0.9×10^{-6}	mm/mm/°C
			α_{22}	54.0×10^{-6}	mm/mm/°C
Glass transition temperature			T_g	203	°C
Curing Temperature			T_C	180	°C
Actual temperature difference used			ΔT_{ACTUAL}	-155	°C

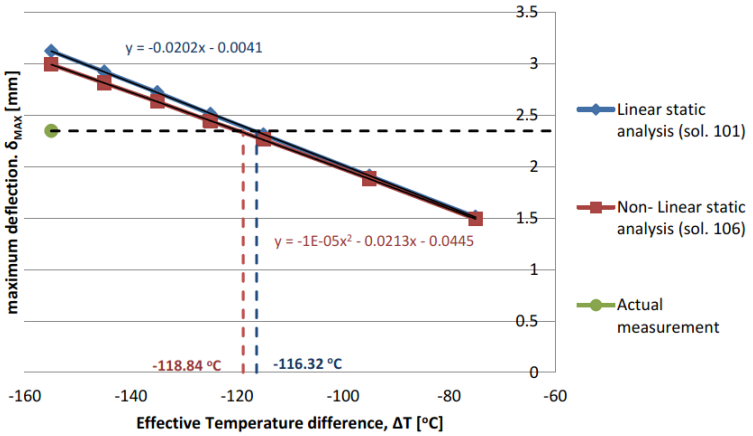

Figure 4: Convergence of deflections with change of temperature difference.

After running both Linear and Non-linear analysis on the model, the Figure 4 shows the relationship between the maximum deflections of laminate at various temperature differences (ΔT) when modelled using Finite Element Analysis. The results suggested that there are strong correlations between the data analysed by each of method of the analysis. The data obtained by linear static analysis can be presented a linear function while as the Non-linear analysis using polynomials of degree 2. It can also be seen that the differences in the maximum deflection between the results obtained from the two analyses become bigger as the ΔT value increases.

According to the experimental measurements, the maximum deflection at the corner of the laminate was measured to be at 2.34mm. By running the FE model with different ΔT, the corresponding effective temperature difference ΔT_{ETD} was able to be found as,

Linear Static analysis ΔT = -116.32°C

Non-linear static analysis ΔT = -118.84°C

It is interesting to see that if the analysis was run without calibration of the data, the resulting difference between the FEA results and the actual laminate would be as great as 33.0% for the maximum deflection obtained through linear static analysis and 27.5% for the non-linear analysis. The errors of the analysed results through using the effective temperature difference ΔT_{ETD} are reduced to less than 5%.

3.2 Stiffened panel

The material and the skin layup for the stiffened panel model are the same as the unsymmetrical laminate, whereas the stacking sequence of the stiffener is $[45/-45/0_3/90/0_3/-45/45]$.

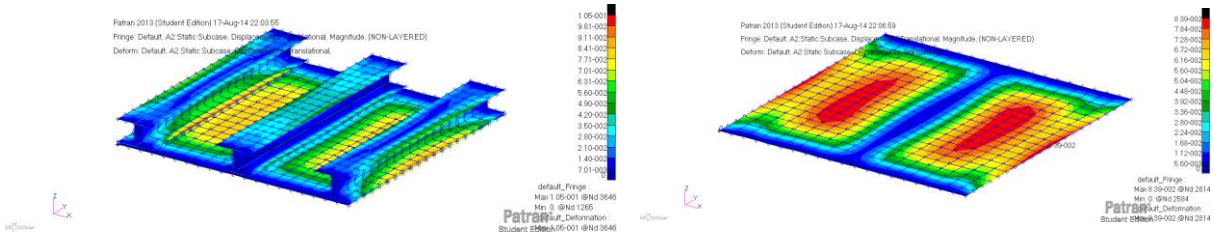

Figure 5 Fringe plotting of the deflection [mm] for Case 1 constraints.

Figure 5 indicates that the stiffened panel under case 1 constraint has a maximum displacement of 0.106 mm which occurs at the stiffener flanges and the maximum out-of-plane deflection for the panel of 0.0839mm. This is because stringers consists of thinner laminate and so will experienced relatively larger deflections when subjected to equal amount of thermal cooling. The maximum deflection of the

panel occurs at the unattached region at which there is no extra stiffness contributed by the stringers on the panel. When the panel are allow to deform in the longitudinal direction (Y direction) along one of the edges, the out-of-plane displacement of the panel increases 57.3% from 0.0839 to 0.132mm. This is because the panel is allowed to contracts as the temperature drops resulting in a larger strain level and with a presuming lower stress level.

Table 2: Maximum/Minimum stress within the skin laminate

	X [MPa]		Y [MPa]		XY [MPa]	
	Max	Min	Max	Min	Max	Min
Case 1 constraint	75.1	-107	60.1	52.5	4.4	-4.47
Ply (Global ID)	-45 (16)	0 (15)	45 (1)	90 (13)	0 (15)	0 (15)
Case 2 constraint	58.6	-99.4	59.4	51.8	3.97	-4.09
Ply (Global ID)	-45 (3)	0 (15)	45 (1)	-45 (16)	0 (13)	0 (15)

The maximum and minimum thermal stress in the skin laminate from Case 1 and Case 2 constraint are summarize in Table 2. The stress values for the stringers were not included as it is considered to be varying upon the geometry and the thickness. The highest stress tends to occur in the ±45° plies at which developed a high tensile stress while as high compressive stress occurs in 0° plies. In general, there are no great variation of stress level in the Y-direction between the plies and the values lies between small ranges where the stress occurs in the range of 50 - 60 MPa. Additionally, the shear stress is considerably low when compared with another 2 components and that the maximum shear stress occurs at the 0° plies. In accordance to the results obtained, there is no significant difference in the stress value within the laminate as when the constraint 1 and 2 were assigned. Although the stresses for the Case 1 are generally higher due to the limitations in the strains, this is still considered a relatively small increase. The difference in the maximum X-component stress (tensile) is calculated to be 24.68% and 8.1% for the Min. stress (compressive) between Case 1 and 2 constraints.

3.3 Wing structure

The same material properties as the unsymmetrical laminate model were used in the wing model and the stacking sequence for each component is listed in Table 3.

Table 3: Stacking Sequences of components for the wing structure

Component	Stacking sequences	Ply % [0,45,-45,90]	Thickness [mm]
Stringer	[+45/-45/0_3/90/0_3/-45/45]	[50, 16.7, 16.7,16.7]	3.132
Skin	[±45/90/45/0_2/-45/0_2]s	[44.5, 22.25, 22.25, 11]	4.698
Spar Web	[±45/90/45/0_2/-45/0_2]s	[44.5, 22.25, 22.25, 11]	4.698
Spar Flange	[±45/90/0_3/90/0_2]s	[55.6, 11.1, 11.1, 22.2]	4.698
Rib	[±45/90/±45/±45/0]s	[12.5, 37.5, 37.5, 12.5]	4.176

After running the FE model of the wing structure with different boundary conditions, it was found that the free constraints – Case 3 gives rise to the largest overall deflection of 59 mm, as shown in Fig 6, which is actually 6 times larger when compare with Case 1 the wing root clamped and 11 times of Case 2 constraint with the spars clamped. However, there are no significant local deflection shown in the components as what is presented in Case 2 in the particular region of the skin and ribs.

For the thermally-induced residual stress of Case 1 and 2 constraints, it was observed that despite the maximum stress presented in the wing model, most of the wing region have a moderate stress value and that the high stress values only occurs near the constrained region, around the wing joint region. This indicates that the excessive boundary conditions were assigned to the model causing unfavourable stress concentration in the local regions. This is a detrimental effect which will leads to delamination of the plies following by the structural failure.

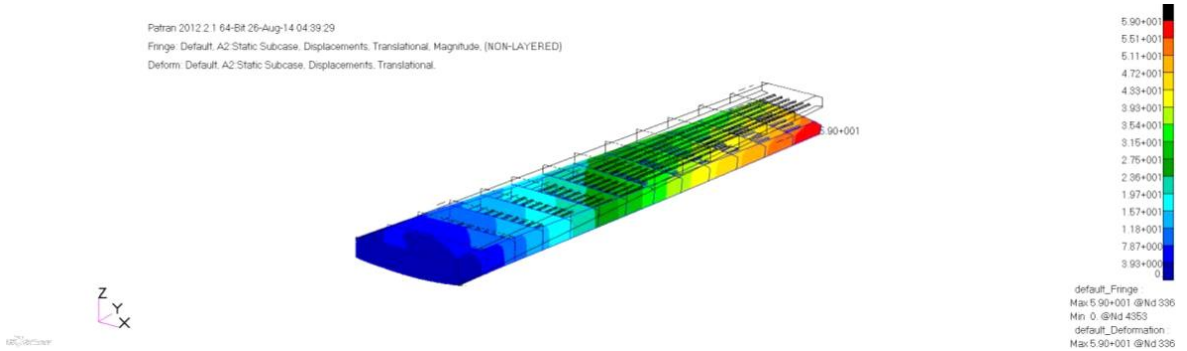

Figure 6: Fringe plotting of the full wing deflection for boundary condition Case 3.

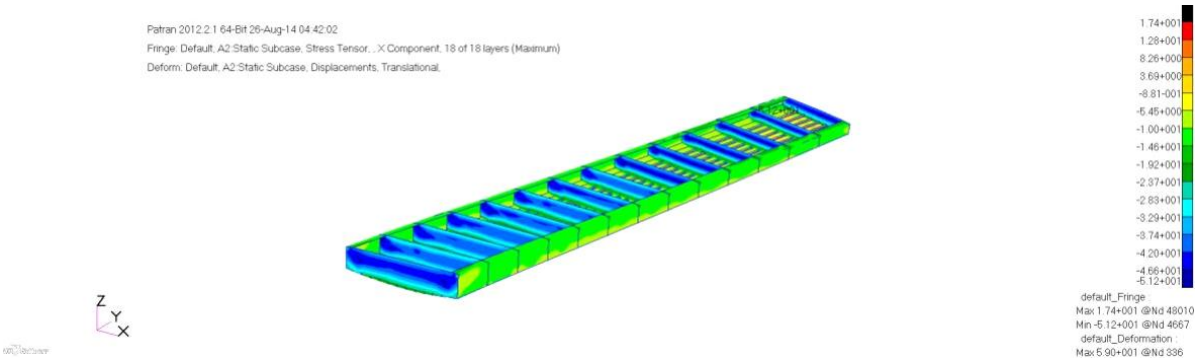

(a)

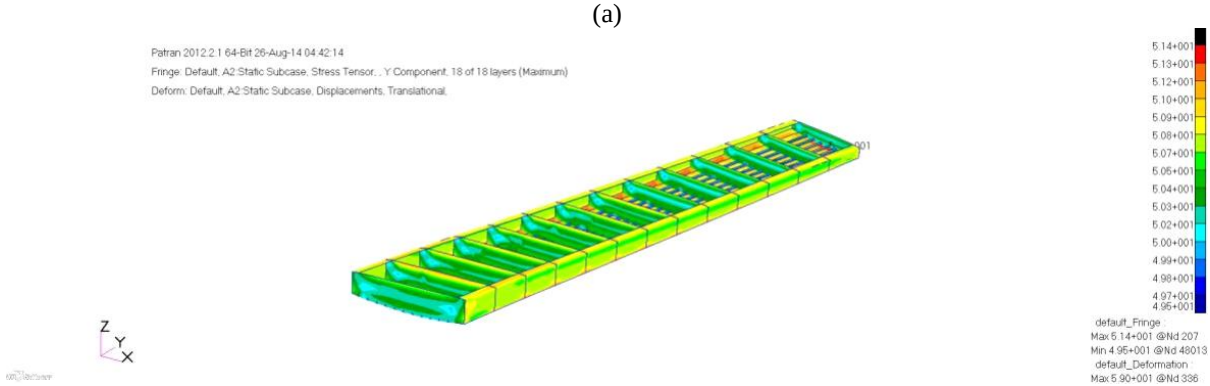

(b)

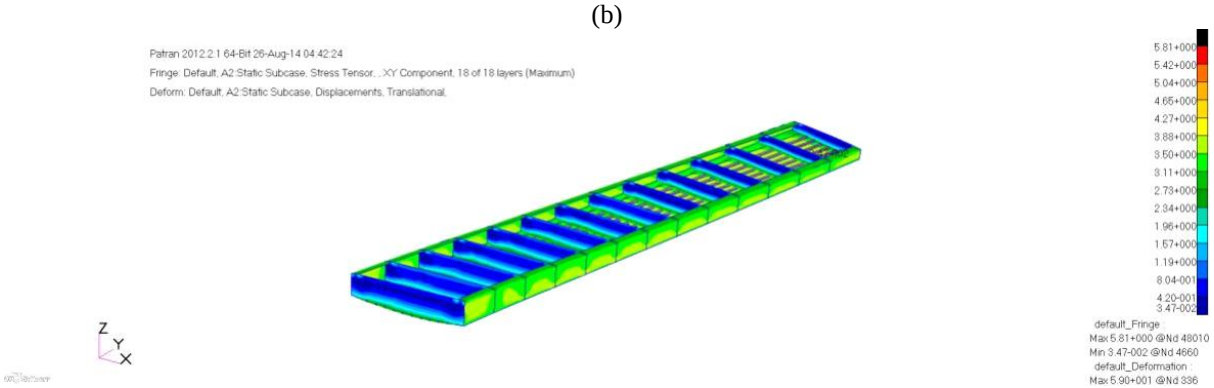

(c)

Figure 7: Fringe plotting of the thermal residual stress of the full wing (a) X-component, (b) Y-component, (c) XY-component for Case 3 constraint.

On the other hand, Case 3 constraints give better overall stress results, as shown in Fig. 7. There are no local stress concentrations due to the applied boundary conditions. As usual, the most critical stress in consideration is the X-components stress at which most of the wing structure undergoes a

compressive stress. The highest compressive stress occurs in the rib at which the stress value is -51.2 MPa whereas the other components such as the spars and the skin panel have the value of around -20 MPa. The maximum tensile stress only appears in the stringer web, along the free edge. The Y-component stress exists in a narrow range between 49.6 to 51.4 MPa. The maximum Y-component stress occurs at the spar flange at which it is attached to the skin. This is because when compares the relative stiffness and the CTE of the spar flanges with the skin, as the spar flanges consist of more 0 degree plies, the stiffness of the laminate will be relatively higher and that the CTE will be lower. When it is attached to the skin, they must both shared the same common strain level at which in general, the skin laminate would be expected to have greater thermal strain if allow to be freely deformed. It can be concluded that the greater the relative difference of the 0° plies within the two laminates, the larger stress level developed within them.

4 CONCLUSIONS

In order to construct the FEM to simulate the thermal residual stress and the panel deflection due to thermal strain, calibration curve was determine in order to obtained the desired ΔT_{ETD} value which will results in the expected panel deflection.

The stringer should be model using two dimensional elements in order to simulate appropriate stiffness as well as clearly representing the stress behaviour within the laminate due to structural interactions between the skin and the stringers. By constraining the stringer's end, even though this result in an increase in thermal residual stress within the laminate by 28.63%, it is consider more favourable than allowing one of the end to freely deform as it reduces the panel deflection by 57.3%.

For the full wing analysis, 3 different cases of boundary conditions are studied. It is observed that the if the CFRP wing are to be co-cured in the autoclave at which the structure are to be clamped at one end of the spars (Case 2), this will leads to a lowest deflection in the final structure. However high stress level will be developed. Despite the fact, if the whole side of the wing structure is to be clamped (Case1), the maximum deflection doubles and that the maximum thermal stress developed decreases by more than half. It is therefore depends on the manufacturer whether they will required the final product to be more accurate in dimensions with higher thermal stress or lower stress with greater deflections. In another hand, Case 3 representing the freely deformed wing model will be an ideal case as there is no local stress concentrations developed inside the structure. However, the maximum deflection achieved is considerably high at which it might not be appropriate in terms of the precision level of the final product.

REFERENCES

[1] M.R. Wisnom, M. Gigliotti, N. Ersoy, M. Campbell and K.D. Potter, 2006, Mechanisms generating residual stresses and distortion during manufacture of polymer–matrix composite structures, Composites Part A: Applied Science and Manufacturing, Volume 37, pp. 522-529.

[2] M.L. Dano, and M.W. Hyer, 1998, Thermally-induced deformation behavior of unsymmetric laminates, lnt..L Solids Structures, 35(17), pp. 2101-2120.

[3] G. F. Carolyne Albert, 2002. Spring-in and warpage of angled composite laminates, Composites Science and Technology, Volume 62, pp. 1895-1912.

[4] Y. Zhang, Z. Xia, Z. and F. Ellyin, 2004, Evolution and influence of residual stresses/strains. Composites Science and Technology, Volume 64, p. 1613– 1621.

[5] J.A.H Magnus Svanberg, 2004, Prediction of shape distortions Part I. FE-implementation of a path dependent constitutive model, Composites Part A: Applied Science and Manufacturing, 35(6), p. 711–721.